Compensation of Doppler Effect in Direct Acquisition of Global Positioning System using Segmented Zero Padding

H. Amiri, and H. Khaleghi Bizaki

Electrical and Electronic Eng. Department, Malek Ashtar University of Technology,
hossein756@yahoo.com, hbizaki@gmail.com
Corresponding author: hbizaki@gmail.com

Abstract*- Because of the very high chip rate of global positioning system (GPS), P-code acquisition at GPS receiver will be challenging. A variety of methods for increasing the probability of detection and reducing the average time of acquisition have been provided, among which the method of Zero Padding (ZP) is the most essential and the most widely used. The method using the Fast Fourier Transform (FFT), searches phase codes of the uncertainty region in a parallel method to find the desired code for correct acquisition. ZP method is sensitive to Doppler frequency so that the increase in Doppler frequency drastically reduces the probability of detection and consequently the average time of acquisition increases. The presented method in this paper, that called Segmented Zero Padding (SZP), reduces the Doppler effects on probability of detection at the acquisition of GPS receiver. Also, it will be shown that using the proposed algorithm proper mean acquisition time at high Doppler frequencies is achievable. Based on the comparisons made in this paper, we prove that the proposed algorithm in comparison to ZP algorithm, maintains the capability of parallel search and finally has a lower average acquisition time.

***Index Terms*- Segment Zero Padding (SZP), Zero Padding (ZP), Direct Average Method (DAM), Probability of Detection, Average Acquisition Time; Global Positioning System (GPS).**

I. INTRODUCTION

In global positioning system two types of PN codes have been used: One is known as the C/A code and the other is known as P code. The period of C/A code is approximately 1 millisecond and the transmission rate is 1.023 Mega chips per second, while the period of P-code is approximately 7 days, and the transmission rate is 10.23 Mega chips per second. C/As are standard codes that are used in general navigation systems and are accessible for public while P-code is very accurate and is used for military purposes [1]. P code acquisition is mainly performed through acquisition of C/A code. Due to the vulnerability of the C/A code to jammer, interference and eavesdropping, acquisition of P-code

would be vulnerable, too. Thus, the direct P-code acquisition methods have been highly regarded. P-code has a very long period, thus the area of uncertainty will be very large and acquisition operations will be increased drastically [2]. Many methods proposed in literatures have two main aspects: reducing the acquisition time with a faster search method and/or reduction of the area of uncertainty region. In the first aspect, the acquisition process can be implemented in parallel, serial or hybrid methods. Parallel methods search the phase codes of the uncertainty area in parallel way to achieve the correct phase codes that, due to the very long spreading code in P-code, have some limitations in hardware implementation. [3] Serial search method that searches phase codes one by one will be very slow due to the large volume of the uncertainty space [4]. Hybrid methods that have created based of trade-off between the parallel and serial methods have been more attractive. In these methods, a segment of code phase is searched in parallel. Zero Padding (ZP) method is one of the most commonly used in which segments of code phase are searched in parallel using FFT [5]. In the second aspect, the methods have been suggested for reducing the uncertainty space, which are based on the mapping of several phase codes to one phase code. It should be noted that, the second aspects could be improved by use of the fast searching methods such as ZP. Direct Average Method and XFAST are examples of these methods [7], [6]. The basis of ZP method is as follows: (1) Addition of N/2 zeros to N/2 samples of the sampled received signal to form a sequence of length N, and then the calculation of the corresponding N-point complex-conjugate FFT. (2) The calculation of the N-point complex-conjugate FFT of N samples of the local spreading codes that have been generated in the receiver. (3) Calculation of the sample by sample multiplication of the results of step1 and step2, and then the calculation of the inverse N-point FFT. N/2 of the first sample resulting from steps 3 shows the correlation result of N/2 samples of sampled received signals and N samples of spreading codes, therefore in ZP method whenever the algorithm is run, the N/2 phase codes can be searched in parallel using an N-point FFT. As a result, N represents the parallel search capability of ZP algorithm. The larger N, the more the number of phase codes searched in each run of ZP algorithm and consequently less average time of acquisition. However, as N increases, a higher amount of Doppler frequency is entered to the correlation calculation process which in turn decreases the probability of detection. If N is equal to one period of Doppler frequency, then the maximum degradation takes place in correlation calculation [8]. Thus, the maximum value for N should be less that the Doppler period. On the other hand, as N decreases the parallel search capability of system reduced and consequently the average time of acquisition increases which in turn reduces the acquisition system performance. The comparison between the detection probability and average time of acquisition of the ZP and the proposed algorithms (called SZP) shows that our algorithm without losing the probability of detetion at high Doppler frequency can achieve high parallel search capability. According to the estimated Doppler frequency, the proposed method segments the maximum parallel search capability (i.e. N) of acquisition in a way that the effects of the Doppler frequency to be minimized as described below.
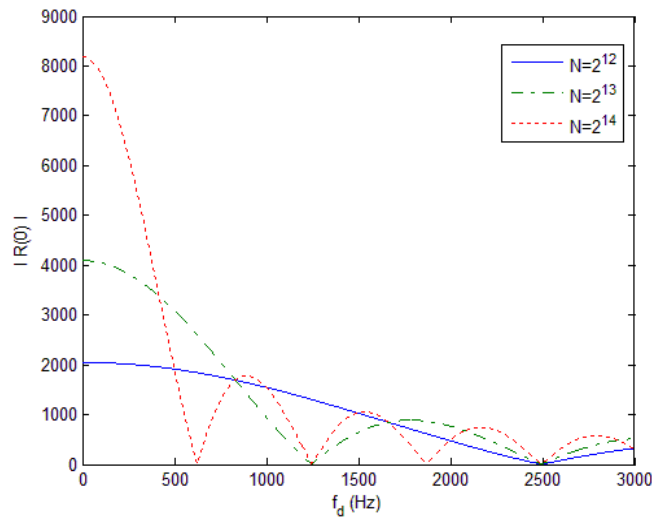
Fig. 1. The maximum correlation as a function of Doppler frequency shift

First, in order to understand the damaging effects of Doppler frequency on correlation of spreading code, an example is given. Suppose the baseband received signal is as follows:

$$x_l = Ac_{l+\lambda}\cos(2\pi f_d l\Delta t + \varphi) + n_l \; ; l = 0,1,2, \ldots \tag{1}$$

Where A is the amplitude of the received signal, C is the spreading code, λ is the phase of spreading code, f_d is Doppler frequency, l is the sample number, Δt is the time interval of each sample (chip time) and φ the phase of the received signal and n is the cumulative noise with mean of zero and a variance of σ^2. For simplicity, we assume the noise less case, n=0, the signal amplitude is one, A = 1 and the initial phase of the signal is zero, φ = 0. Cross correlation R (τ) is defined as the correlation between the received signal, with a length of N/2 samples, and local spreading code of c ($l + \lambda + \tau$) then the (auto-)correlation is:

$$R(0) = \sum_{l=0}^{N/2} c_{l+\lambda}{}^2 \cos(2\pi f_d l\Delta t) = {\sin(\pi f_d N\Delta t)}\Big/{(\pi f_d N\Delta t)} = \frac{N}{2}sinc(f_d N\Delta t) \tag{2}$$

Equation (2) calculates the peak of correlation or auto-correlation. As can be seen, this peak is dependent on Doppler frequency. In order to demonstrate the Doppler Effect on autocorrelation, assume Δt = 1/ (10.23 × 10⁶) second. Fig. 1 displays R (0) as a function of Doppler frequency with different values of N. As can be seen, when N=2¹² the maximum loss is occurred at a frequency of 2.5KHz, However, as N increases up to 2¹⁴, the highest loss in auto-correlation is occurred at a frequency of approximately 0.6KHz. This imply that by increasing the N, sensitivity to Doppler frequency is also increased.

In this paper, with using the proposed algorithm the sensitivity to the Doppler frequency due to increasing the value of N will be minimized and the results will be compared with those of ZP method. In the section II SZP algorithm will be described generally. In the section III, the

mathematical model of the algorithm is described to make comparison with ZP method and in the section IV with a numerical example, the SZP algorithm will be compared with ZP algorithm and in section V the algorithm will be modified for the correlation peak of the detection probability and the average time of acquisition.

II.   SEGMENTED ZERO PADDING ALGORITHM

SZP algorithm is equivalent to segmented matched filters in the frequency domain [8]. SZP algorithm similar to ZP algorithm searches phase codes of uncertainty space in parallel. Fig. 2 shows the block diagram of the algorithm. SZP algorithm is based on dividing the parallel search block (or simply the parallel search capability of N system hardware) into equal subsets (N_s, the subset number) and then calculating parallel search on each subsets. According to Fig. 2, if the local spreading code with the period L called C and samples of received signal at the chip rate called x, then the SZP algorithm will be as follows:

1.   Select N/2 samples from the beginning of the local spreading code. $C_1 \sim C_{(N/2)}$

2.   Select N/2 samples of the received signal sampled at the chip rate. $x_1 \sim x_{(N/2)}$

3.   Divide N/2 samples of section 2 into N_s equal subsets that the number of samples in each subset is equal to $N / (2N_s)$.

4.   Add $N / (2N_s)$ zero (sequence $0_{(1 \times N / (2Ns))}$) to the end of subsets of section 3 to reach the size of N / N_s.

5.   Run ZP algorithm for each subset of N/N_s samples from section 4 and the corresponding code. Code corresponding to each subset is identified with hachure in figure, and for example the word ZP_i means ZP algorithm run for the i_{th} subset and the result for each subset, is $N/ (2N_s)$ samples of correlation between the i_{th} subset and the corresponding local code that is marked with the letter Z. $Z_{i,j}$ means the j_{th} sample of correlation from the i_{th} subset.

6.   Square all samples of section 5, and sum up samples with the subscript j, the correlation between $N / (2N_s)$ samples of the sampled received signal and $N / 2$ spreading codes are obtained

7.   If any of the $N / (2N_s)$ samples of section 6 exceeds the threshold, the acquisition process stops and the process is sent to tracking step, and if not, $N / (2N_s)$ to left shift the spreading code and the steps will be repeated from section 5.

Fig. 3 shows flowchart of SZP algorithm. As mentioned in section 6 for each run of SZP algorithm, $N / (2N_s)$ phase codes are searched in parallel. As the number of sections increases, the number of phase codes searched at the every run of the algorithm is reduced. This is a disadvantage for the algorithm, when the Doppler frequency is zero that the ZP algorithm is able to search N/2 phase codes in parallel with the same amount of computations. In the third section, we will show that as the

Doppler frequency increases, the probability of detecting in ZP algorithm greatly decreases while the SZP algorithm resists to Doppler frequency increases and prevents the loss of detection probability.
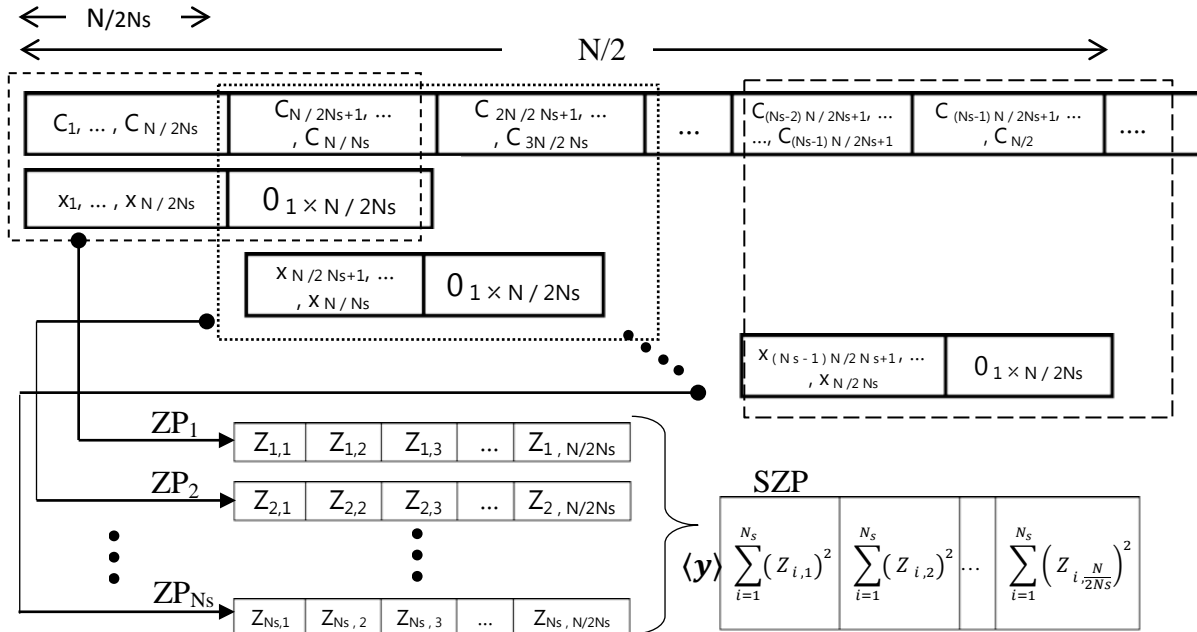

Fig. 2. SZP block diagram

III. PREPARATION OF MATHEMATICAL MODEL AND SZP ALGORITHM EFFICIENCY ASSESSMENT

In this section in order to compare SZP with ZP algorithms, its mathematical model is presented and then the probability of detection and false alarm and the average time of acquisition are calculated.

A. Mathematical model of the algorithm

Suppose the received baseband signal after Analogue to digital converter of GPS receiver is as follows:

$$x_l = x_{I,l} + j x_{Q,l} \, , (l = 0,1,2, \dots .) \tag{3}$$

where,

$$x_{I,l} = S d_{l+\tau} c_{l+\tau} \cos(2\pi f_d \Delta t \, l) + n_{I,l} \tag{4}$$

$$x_{Q,l} = S d_{l+\tau} c_{l+\tau} \sin(2\pi f_d \Delta t \, l) + n_{Q,l} \tag{5}$$

where S is the signal amplitude, d is the transmitted data, C is the spreading code considered here as the P-code, f_d is Doppler frequency offset, and τ is the initial phase of the spreading code and l is the counter of the samples. $n_{I,l}$ and $n_{Q,l}$ indicate the real and imaginary parts of noise with a mean of

zero and a variance of σ^2, Therefore, the received SNR will be as $S^2 / 2\sigma^2$. Given that the GPS data transmission rate is 50 bps, d can be assumed constant and equal to one in the process of acquisition. [1].
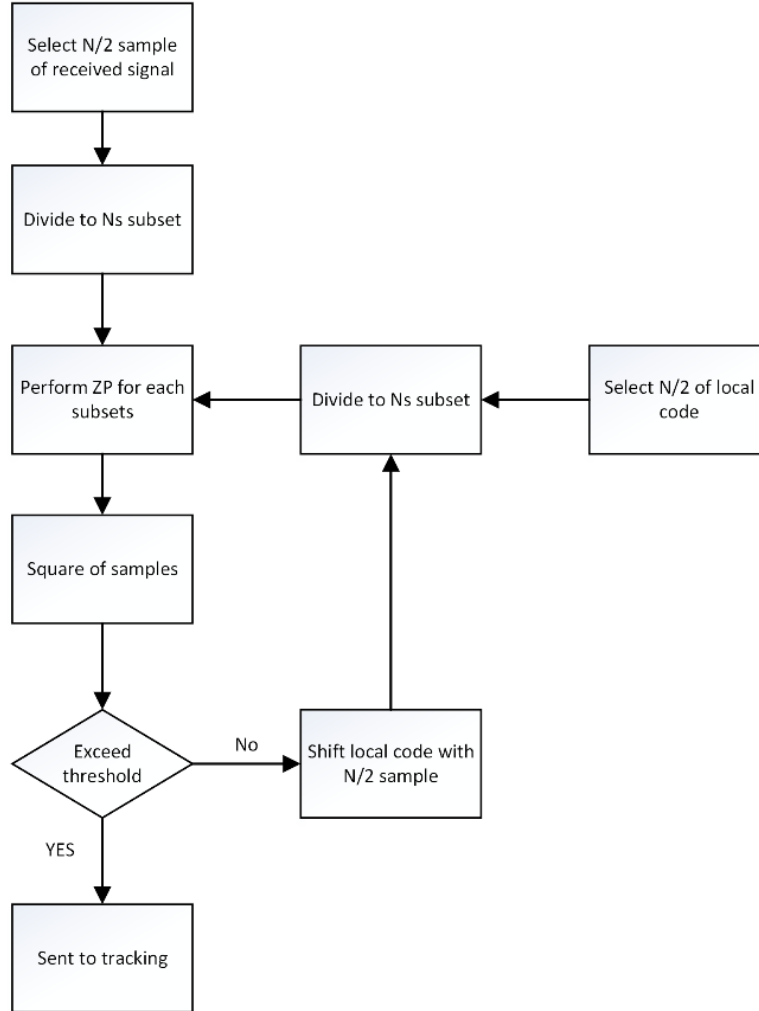

Fig. 3. Flow chart of segmented zero padding

B. *Detection probability, false alarm and threshold*

To calculate the probability of detection in the acquisition process, Statistical properties of the spreading code and autocorrelation and cross-correlation properties must be examined. According to Fig. 2, if the correlation output of the ith subset from N_s subsets of the received signal in phase with (4) and with the spreading code of c $_{(l + \mu)}$ (μ represents the initial phase of the local spreading code) is shown as$Z_{i,j}^l$, then:

$$Z_{i,j}^I = \sum_{l=\frac{N(i-1)}{2N_S}+1}^{\frac{Ni}{2N_S}} Sc_{l+\tau+j}\cos(2\pi f_d \Delta tl)*c_{l+\mu} + \sum_{l=\frac{N(i-1)}{2N_S}+1}^{\frac{Ni}{2N_S}} n_{I,l}*c_{l+\mu} = W_{i,j}^I + V_{i,j} \tag{6}$$

In (6) $W_{i,j}^I$ represents the result of the coherent integration of the in-phase received signal and the spreading code. The average of $W_{i,j}$ is equal to:

$$E_{W_{i,j}^I} = SR_m \sum_{l=\frac{N(i-1)}{2N_S}+1}^{\frac{Ni}{2N_S}} \cos(2\pi f_d \Delta tl); m = 0,1 \tag{7}$$

where, $m=0$ represents false hypothesis and is displayed by H_0 and $m=1$ represents the correct hypothesis and is displayed by H_1. R_m is the normalized autocorrelation function of the spreading code that is zero at H_0 and is equal to one at H_1 [9]. $W_{i,j}^I$ Variance has an upper bound of $S^2 \frac{N}{2N_S} G_m$ where, $G_m=1-R_m$ [9]. For a very large group of spreading codes, according to the central limit theorem $W_{i,j}^I$ is a random process with normal distribution [9]:

$$W_{i,j}^I \sim \mathcal{N}\left(E_{W_{i,j}^I}, S^2 \frac{N}{2N_S} G_m\right); m = 0,1 \tag{8}$$

For $V_{i,j}$ with respect to the fact that the spreading code and the noise are independent, $V_{i,j}$ is a normal process with zero mean and a variance of $\sigma^2 \frac{N}{2N_S}$. As a result, (6) is a random process with normal distribution as follows:

$$Z_{i,j}^I \sim \mathcal{N}\left(E_{W_{i,j}^I}, \Sigma_Z^I\right); m = 0,1 \tag{9}$$

where,

$$\Sigma_Z^I = \frac{N}{2N_S}(S^2 G_m + \sigma^2); m = 0,1 \tag{10}$$

According to Fig. 2, if the final output of the algorithm for calculating the correlation between the in-phase received signal and the spreading code is shown as $\langle y^I \rangle$. Then $\langle y^I \rangle$ at any run of the algorithm will have $\frac{N}{2N_S}$ samples which are sum of squares of N_s values of random process normally distributed as in (9). $\langle y_k^I \rangle$ also refers to the k_{th} member of $\langle y^I \rangle$ and is written as follows:

$$\langle y_k^I \rangle = \sum_{j=1}^{N_s} (Z_{k,j}^I)^2 ; 1 \le k \le \frac{N}{2N_S} \tag{11}$$

Similarly, for the vertical mode we have:

$$Z_{i,j}^Q \sim \mathcal{N}\left(E_{W_{i,j}^Q}, \Sigma_Z^Q\right); m = 0,1 \tag{12}$$

where,

$$\Sigma_Z^Q = \Sigma_Z^I = \frac{N}{2N_S}(S^2 G_m + \sigma^2); m = 0,1 \tag{13}$$

$$E_{W_{i,j}^Q} = SR_m \sum_{l=\frac{N(i-1)}{2N_S}+1}^{\frac{Ni}{2N_S}} \sin(2\pi f_d \Delta t l); m = 0,1 \tag{14}$$

And

$$\langle y_k^Q \rangle = \sum_{j=1}^{N_s} (Z_{k,j}^Q)^2 \; ; \; 1 \le k \le \frac{N}{2N_s} \tag{15}$$

At the receiver, the result of two in-phase and Quadrature sets are sent to the envelope detector after the correlation operation [10]:

$$\langle \gamma_k^Q \rangle = \langle y_k^I \rangle + \langle y_k^Q \rangle \tag{16}$$

Equation (16) is varied based on the true or false assumption and for simplicity of the following calculations, it will be assumed that the amplitude of the received signal is equal to one (S = 1):

1. H_0 hypothesis:

In this case, the result of the (7) and (14) will be zero and (16) consists of the sum of squares of $2N_s$ normal process with zero mean. Since the distribution of the total sum of a number of squared standard and normal variables is a Chi square distribution [11] and because all $2N_s$ processes have the same variance of $\Sigma_Z^Q = \Sigma_Z^I$, the random variable $\eta = \frac{1}{\sqrt{\Sigma_Z^Q}}\gamma$ can be defined. In this case η includes $2N_s$ squared standard and normal processes with Chi square distribution and $2N_s$ degrees of freedom. Finally, the random variable γ using $\gamma = \eta\sqrt{\Sigma_Z^Q}$ has a gamma distribution as $\gamma \sim \Gamma(k, \theta)$, that, $k = N_S$ and $\theta = 2\Sigma_Z^Q$ are its parameters [11]. The probability density function of the gamma distribution is as follows:

$$f_\gamma(t|H_0) = \frac{t^{k-1} e^{-\frac{t}{\theta}}}{\theta^k \Gamma(k)} , t > 0, k, \theta > 0 \tag{17}$$

where $\Gamma(k)$ is the gamma function. Cumulative distribution function for the gamma distribution is as the following equation:

$$F_\gamma(t|H_0) = \frac{\vartheta(k, \frac{t}{\theta})}{\Gamma(k)} \tag{18}$$

where $\vartheta(k, \frac{t}{\theta})$ is the incomplete gamma function. Using (18) false alarm probability can be calculated for a searching phase code as follows [4]:

$$P_{fa}^{(cs)} = 1 - F_\gamma(V_t|H_0) \tag{19}$$

where, V_t is threshold. Finally, using (19) the threshold is calculated as follows:

$$V_t = F_{\gamma}^{-1}\left(\left(1 + P_{fa}^{(cs)}\right), k, \theta \middle| H_0\right) \tag{20}$$

2. H$_1$ hypothesis:

In this case, the result of (7) and (14) is not zero and (16) will include the sum of the squares of 2N$_s$ normal processes. If the new random variable η is defined as $\eta = \dfrac{1}{\sqrt{\Sigma_Z^Q}}\gamma$, η includes 2N$_s$ squared normal processes with non-zero mean and unit variance, which has Noncentral Chi Square distribution with 2N$_s$ degrees of freedom as follows [11]:
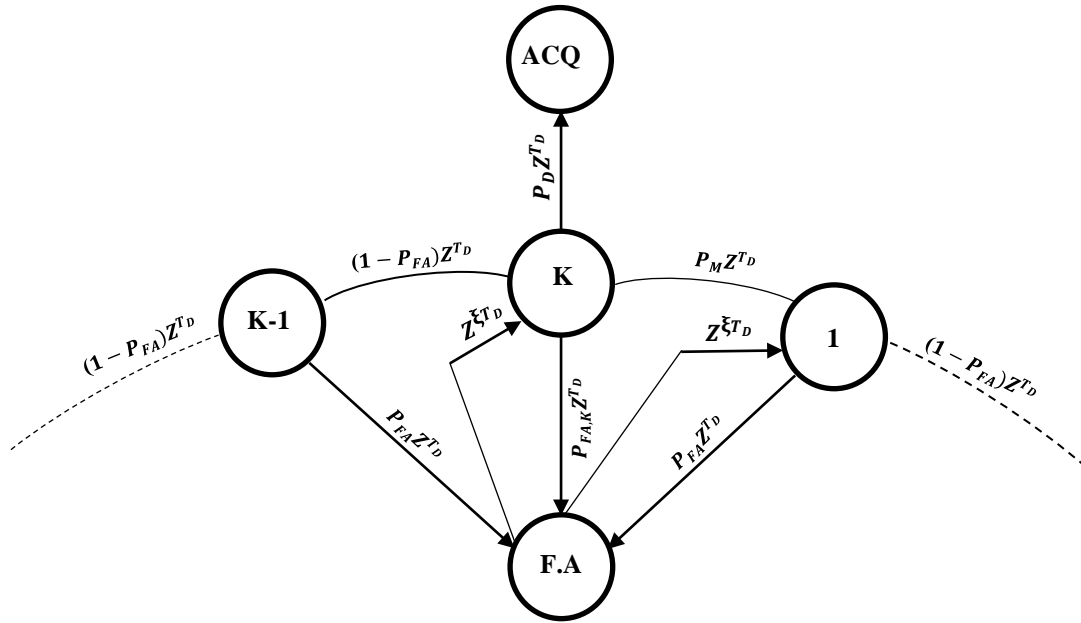

Fig. 4. Flow graph diagram of SZP algorithm

$$\eta \sim \chi_{2N_S}^{`2}(\mu^2) \tag{21}$$

where μ^2 is called the distribution parameter and is calculated by the following equation:

$$\mu^2 = \sum_{i=1}^{N_S}\left(\left(\frac{E_{W_{i,j}^I}}{\sqrt{\Sigma_Z^Q}}\right)^2 + \left(\frac{E_{W_{i,j}^Q}}{\sqrt{\Sigma_Z^Q}}\right)^2\right) = \frac{1}{\Sigma_Z^Q}\sum_{i=1}^{N_S}\left(E_{W_{i,j}^I}^{\ 2} + E_{W_{i,j}^Q}^{\ 2}\right)$$

$$= \frac{1}{\Sigma_Z^Q}\sum_{i=1}^{N_S}\left(\left(\sum_{l=\frac{N(i-1)}{2N_S}+1}^{\frac{Ni}{2N_S}}\cos(2\pi f_d\Delta t l)\right)^2 + \left(\sum_{l=\frac{N(i-1)}{2N_S}+1}^{\frac{Ni}{2N_S}}\sin(2\pi f_d\Delta t l)\right)^2\right)$$

$$= \frac{N^2}{4N_S\Sigma_Z^Q}\left(sinc\left(\frac{N f_d\Delta t}{2N_S}\right)\right)^2$$

$$\tag{22}$$

Since $\mu^2 \geq 0$ and $N_S > 0$, the distribution of the random variable η can be approximated as a normal distribution with mean and variance as follows [11]:

$$\eta \sim N(2N_S + \mu^2, 2(2N_S + 2\mu^2)) \tag{23}$$

Finally, given that $\gamma = \eta \sqrt{\Sigma_Z^Q}$ the distribution of γ will be also normal:

$$\gamma \sim N(\Sigma_Z^Q(2N_S + \mu^2), 4\Sigma_Z^{Q^2}(N_S + \mu^2)) \tag{24}$$

or,

$$f_\gamma(t|H_1) = \frac{1}{\sqrt{8\pi\Sigma_Z^{Q^2}(N_S + \mu^2)}} \; e^{-\frac{(t - \Sigma_Z^Q(2N_S + \mu^2))^2}{8\Sigma_Z^{Q^2}(N_S + \mu^2)}} \tag{25}$$

and the cumulative distribution function is:

$$F_\gamma(t|H_1) = \int_{-\infty}^{V_t} f_\gamma(t|H_1)dt \tag{26}$$

To search $\frac{N}{2}$ phase codes in parallel using SZP method, N_s sub-groups were formed and $\frac{N}{2N_s}$ phase codes were searched in parallel in each sub-group and subsequently in each observation window (one SZP algorithm run) of SZP algorithm, thus, to search $\frac{N}{2}$ phase codes, SZP algorithm needs to be run N_s times. Thus, each observation window of GZP algorithm in which $\frac{N}{2}$ phase codes are searched in parallel is equal to N_s observation windows of SZP algorithm.

Suppose the number of uncertainty area codes is Θ, then the number of observation windows to search the entire area of uncertainty in SZP method will be equal to $K = \Theta \Big/ \left(\frac{N}{2N_s}\right)$. Fig. 4 shows the flow graph of SZP, assuming that the K_{th} observation window covers the received signal samples. In simple terms the K_{th} states of the flow graph is equivalent to H_1 assumption. T_D is the computing time of an observation window or simply one-run time of SZP algorithm, ξ is equal to the fine (return) time of a false alarm, F.A is equal to the false alarm and ACQ is equal to acquisition mode. If we assume that the process is in k_{th} state, then the probability of detecting is equal to the probability that the decision variable, assuming H_1, is greater than the threshold of (20) and all $\frac{N}{2N_s} - 1$ residual samples of the observation window that are included in H_0 assumption:

$$P_D = \int_{V_t}^{\infty} f_\gamma(t|H_1) \left(F_\gamma(t|H_0)\right)^{N/2N_s - 1} dt \tag{27}$$

If at least one of the $\frac{N}{2N_s} - 1$ remaining samples in the k_{th} observation window that are included in H_0 assumption exceeds the threshold, then the false alarm occurs for the k_{th} mode and the probability is as follow:

$$P_{FA,K} = 1 - \left(1 - P_{FA}^{(sc)}\right)^{N/2N_s - 1} \tag{28}$$

where,

$$P_{FA}^{(sc)} = \int_{V_t}^{\infty} f_\gamma(t|H_0) \left(F_\gamma(t|H_0)\right)^{N/2N_s - 2} F_\gamma(t|H_1) dt \tag{29}$$
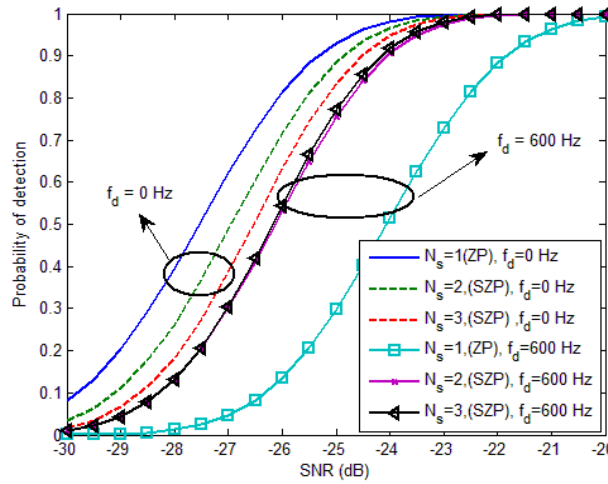

Fig. 5. The probability of detecting to signal-noise ratio for 0 and 600 Hz Doppler frequencies and two different values of N_s

Equation (29) is the probability of false alarm for each $\frac{N}{2N_s} - 1$ sample in the K_{th} mode that are included in H_0 assumption. Equation (28) simply is supplementary to condition in which none of ($\frac{N}{2N_s} - 1$) samples included in H_0 assumption exceeds the threshold. In the K_{th} state, if none of $\frac{N}{2N_s}$ samples exceeds the threshold, then the error occurs and system enters the mode number 1 rather than ACQ mode. The probability of error only occurs in the K_{th} state that is the probability of having neither false alarm nor detection in the K_{th} state:

$$P_M = 1 - (P_M + P_{FA,K}) \tag{30}$$

In K-1 remaining states of flow graph in Figure 2, all of which are included in H_0 assumption, if each of $\frac{N}{2N_s}$ samples of K-1each observation window exceeds the threshold, then the false alarm has occurred and the probability result is calculated as follows:

$$P_{FA} = 1 - (F_\gamma(V_t|H_0))^{\frac{N}{2N_s}} \tag{31}$$

C. Equations, the generating function and the average time of acquisition

Assuming the equal probability of being placed in every K states of the flow graph, then generating function of the flow graph according to [4] can be written as follows:

$$P_{ACQ} = \frac{H_D(z) - H_D(z)H_0^K(z)}{K(1 - H_M(z)H_0^{K-1}(z))(1 - H_0(z))} \tag{32}$$

where,

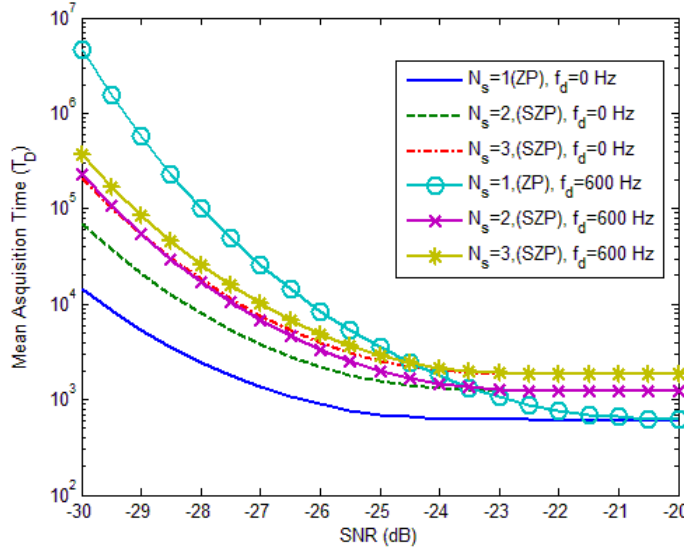$$H_M(z) = P_M z^{T_D} + P_{FA} z^{(K+1)T_D} \tag{33}$$

Fig. 6. The average time of acquisition as a function of the signal to noise ratio for 0 and 600 Hz Doppler frequencies for 3 different values of N_s

$$H_D(z) = P_D z^{T_D} \tag{34}$$

$$H_0(z) = (1 - P_{FA}) z^{T_D} + P_{FA} z^{(K+1)T_D} \tag{35}$$

H_M is coupler path interest of K mode to 1 mode and H_D is coupler path interest of K mode to ACQ mode and H_0 is the interest of all paths except the K_{th} path to the next path. The average time of acquisition using (32) is obtained as follows [4]:

$$E(T_{ACQ}) = \frac{dP_{ACQ}}{dz}\bigg|_{z=1} = \frac{T_D}{P_D}\left\{1 + \xi P_{FA,K} + \frac{(K-1)(1+\xi P_{FA})(2-P_D)}{2}\right\} \tag{36}$$

IV.   COMPARISON BETWEEN ZP AND SZP

To compare SZP algorithm with ZP algorithm, first, we define an acquisition system, then the results obtained will be compared with the results of [12]. For example, suppose the GPS signal with P-code and chip speed of 1.023 Mega chips, a sampling rate of one sample per chip, the total area of uncertainty

includes $\Theta = 10^7$ and a false alarm rate of $P_{FA}^{(sc)} = 10^{-6}$. The maximum FFT length can be calculated by the system is $N = 2^{14}$. Fig. 5 shows the probability of detection versus SNR for both 0 and 600 Hz Doppler frequencies and different divisions. It should be noted that in the case of $N_s = 1$, SZP is the same as ZP, because there is no division. In Fig. 5, in SNR = -26 dB, when the Doppler frequency is zero, detection probability for the ZP algorithm or SZP algorithms with $N_s = 1$ is approximately equal to 0.8, while the probability of detection for the same signal-to-noise ratio and for $N_s = 2$ and $N_s = 3$ at
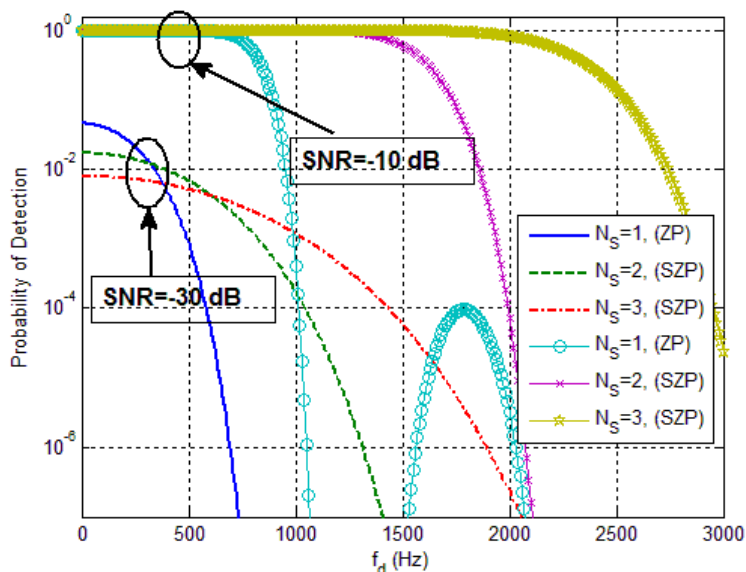

Fig. 7. The probability of detection as a function of the Doppler frequency for signal to noise ratios of -10 dB and -30 dB

zero Doppler frequency is 0.7 and 0.63, respectively. The decrease in the probability of detection at zero frequency is due to loss of the correlation gain [8]. At lower Doppler frequencies, using SZP algorithm reduces the probability of detection and as the amount of divisions (N_s) increases, the loss increases, as well. However, at high Doppler frequencies as can be seen in Fig. 5 for Doppler frequencies above 600 Hz, the situation is different from zero frequency. At SNR = -26 dB for Doppler frequency of 600 Hz, the probability of detection for ZP algorithm is 0.1 and while for the same amount

of SZP algorithm and $N_s = 2$ and $N_s = 3$ are 0.53 and 0.54, respectively, which represents a very good improvement of SZP algorithm for the detection probability. As the Doppler frequency increases by applying SZP algorithm better results for the probability of detection can be achieved while, as the number of divisions increases the improvement of the detection probability becomes less and less or simply the lower divisions, the increased probability of detecting at a constant signal-to-noise ratio.

Fig. 6 shows the average time of acquisition for the system with the detection probability illustrated in Fig. 5. In this figure T_D is equal to the time required for the computations of a single observation window that is equal to parallel search of $\frac{N}{2}$ phase codes in ZP algorithm and $\frac{N}{2N_s}$ phase codes in SZP

algorithm. As a result, for an equal probability of detection, the average time of acquisition in SZP algorithm, is N_s times more than that of the ZP algorithm. As can be seen in Fig. 6, at SNR = -26dB and the Doppler frequency of zero Hz acquisition time of ZP algorithm is lower than that of SZP algorithm with 2 and 3 divisions and at signal-to-noise ratios higher than -21 dB, the probability of detections at the Doppler frequency of zero Hz is approximately as shown in Fig. 5, The average time of acquisition in SZP algorithm with $N_s = 2$ and $N_s = 3$ is respectively 2 and 3 times more than that of the ZP algorithm. However, at Doppler frequency of 600 Hz, the situation is different. As can be seen in Fig. 6 for signal-
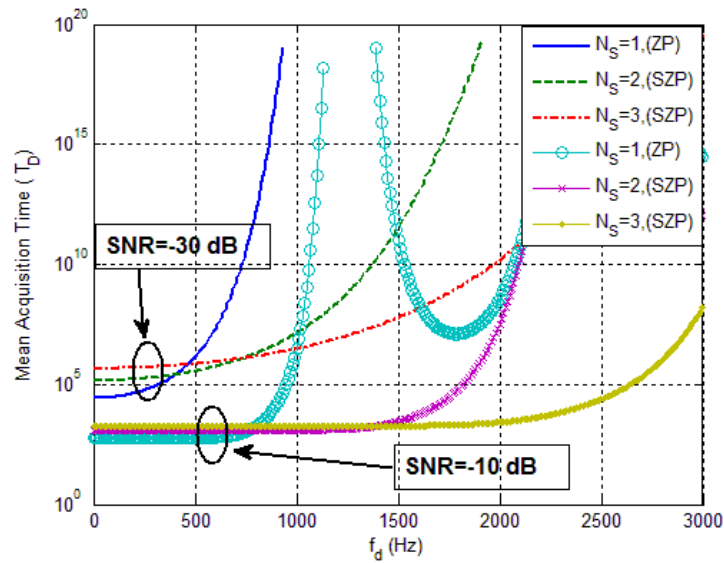

Fig. 8. The average time of acquisition as a function of Doppler frequency, for signal-to-noise ratios of -10 dB and -30 dB in terms of T_D

to-noise ratios below -25dB, the average time of acquisition increases more dramatically in ZP algorithm compared to SZP algorithm when signal to noise ratio decreases, as an example, the average time of acquisition in ZP algorithm at signal to noise ratio of -29dB is 10 times more than the average time of acquisition in SZP algorithm with $N_s = 2$.

In Fig. 6, the values of the average time of acquisition at signal to noise ratios of higher than -21dB has been plotted, where the detection probability of SZP and ZP algorithms are approximately equal to one, at the Doppler frequency of 600 Hertz are converged to Doppler frequency of zero, or in simple words, as the ratio of signal to noise increases the effects of Doppler frequency is reduced so that the average time of acquisition at the presence of Doppler frequency gets equal to that at Doppler frequency of zero. But if the Doppler frequency is so large that of which a period of rotation enters the correlation computations, then performance degradation due to Doppler effect increases so that the average time of

acquisition, even at signal to noise ratios higher than zero, will not reach the average time of acquisition at the absence of Doppler frequency [8]. Fig. 7, for example, shows the probability of detection for the system introduced at the beginning of the section, in terms of Doppler frequency. In

the system having the properties of N=16384 and sampling frequency of 10.23 Mega chips per second, ZP algorithm searches N/2 phase codes or in other words, 8192 phase codes in each observation window, in parallel.

Assuming that an entire period of rotation of Doppler frequency enters the computations, then, the maximum attenuation in detection probability occurs at the frequency of $10.23 \times 10^6 / 8192 \approx 1.2\ KHz$. Thus, a period of rotation of Doppler frequency enters the correlation computations, when Doppler frequency is equal to $f_s/(2N)$. f_s is the sampling frequency.

As shown in Fig. 7, at the signal-to-noise ratio of -10 dB and Doppler frequencies below 1 KHz the probability of detection for ZP and SZP algorithms is approximately equal to one. However, for Doppler frequencies above 1 KHz the detection probability for ZP algorithm drops sharply as the maximum loss

Table I. Complexity value

TITLE	T(D)
N/N$_s$ point FFT of received signal	$\frac{N}{N_s} log \frac{N}{N_s}$
conj of received signal	$2\frac{N}{N_s} + 1$
N/N$_s$ point FFT of local code	$\frac{N}{N_s} log \frac{N}{N_s}$
Multiple revived FFT and local code FFT	$2\frac{N}{N_s} + 1$
IFFT of result	$\frac{N}{N_s} log \frac{N}{N_s}$
Square of result	$\frac{N}{2}$
Sum of result	$\frac{N}{2}$

occurs at the frequency of 1.2 KHz and signal detection is impossible. While the detection probability for SZP algorithm with $N_s = 2$ at higher frequencies is faced with maximum attenuation, as give the division performed, the division (in terms of sample) length is smaller than the original length with no division and as a result, the Doppler frequency must be greater to apply a full period. Thus, the maximum attenuation in the SZP algorithm occurs at a frequency of $f_s N_s / (2N)$. Fig. 7 shows the average time of acquisition for the system shown in Fig. 8.

Based on the Fig. 4, the flowchart and the complexity of each block can be reported as table 1. Thus, total complexity of SZP algorithm is:

$$T(D)_{SZP} = 2\frac{N}{N_s} log \frac{N}{N_s} + \frac{4N}{N_s} + N + 2 \tag{37}$$

By substitution of N$_s$=1, we have the ZP algorithm with the complexity of:

$$\tag{38}$$

$$T(D)_{ZP} = 2NlogN + 4N + N + 2$$

It should be noted that, In order to search in N code phase, the proposed algorithm should be repeated N_s times. Thus, the complexity would be:

$$T(D)_{SZP} = 2Nlog\frac{N}{N_s} + 4N + N_s(N + 2) \tag{39}$$

$$T(D)_{ZP} = T(D)_{SZP}\big|_{N_s=1} = 2NlogN + 4N + N + 2 \tag{40}$$

As can be seen, by increasing the N_s, the complexity would be increased.

V. DIVISIONS CRITERIA

As shown in Fig. 8, at the signal-to-noise ratio of -10 dB for Doppler frequencies less than 700Hz, ZP algorithm has an average time of acquisition smaller than that of SZP algorithm. But with the
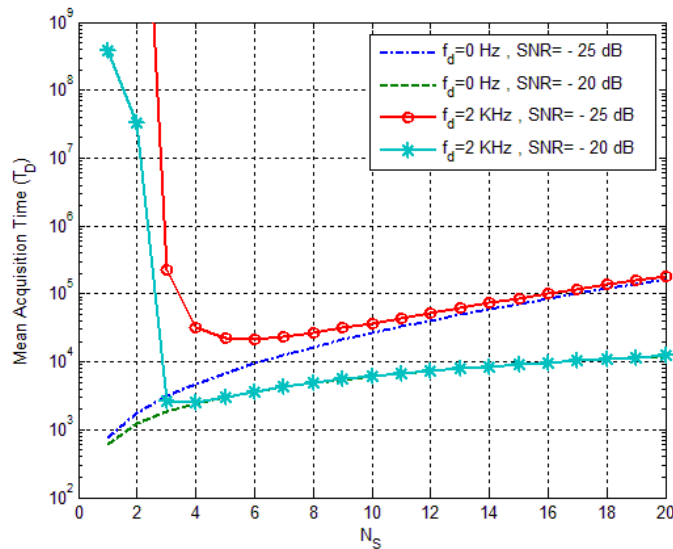

Fig. 9. Average time of acquisition as a function of the number of divisions for
Doppler frequencies of 0 and 2 KHz

increase of Doppler frequency approaching to 1KHz, the average time of acquisition for ZP algorithm is approximately 2500 times more than that of SZP algorithm with $N_s = 2$. At low signal-to-noise ratios,

for example, at signal-to-noise ratio of -30 dB, as shown in Fig. 8, the effects of Doppler frequency on ZP and SZP algorithms is also shown. For frequencies smaller than 400Hz, the average time of acquisition for ZP algorithm is smaller than that of the SZP algorithm with $N_s = 2$ and SZP algorithms with $N_s = 2$ has a smaller average time of acquisition than that of the same algorithm with $N_s = 3$. The reason is that the SZP algorithm by dividing correlation calculations into smaller groups, first, reduces the correlation gain [8] and decreases the probability of detection and second, by reducing the parallel search capacity in relation to the number of divisions, increases the average time of acquisition to the

same degree. As a result, for frequencies less than 400Hz virtually SZP algorithm reduces acquisition system performance with more divisions, because of imposing an extra burden on acquisition system. However, according to Fig. 7, at Doppler frequencies above 400Hz it can be seen that the SZP algorithm with $N_s = 2$ reduces the loss of detection probability and then at around Doppler frequency of 600Hz, SZP algorithm with $N_s = 3$, the probability has higher detection probability rate than that of SZP with $N_s = 2$. Fig. 9 shows the average time of acquisition changes as a function of increase in the number of divisions (N_s). As can be seen, when the Doppler frequency is zero, increasing the number of divisions increases the average time of acquisition. For example, at the signal-to-noise ratio of -25dB the average time of acquisition with $N_s = 3$ is approximately 2 times more than that with $N_s=2$.

However, when the Doppler frequency is 2 KHz, at SNR= -20 dB with increasing divisions from $N_s = 2$ to $N_s = 3$, the average time of acquisition decreases by 12000 times. That confirms the very good performance of our algorithm in the presence of constant Doppler frequency. As mentioned, $N_s = 1$ is equivalent to the ZP algorithm, according to Fig. 9, the average time of acquisition in ZP algorithm is almost 150,000 times more than that of SZP algorithm with $N_s = 4$ at the signal to noise ratio of -20dB, and Doppler frequency of 2KHz.

According to what has been stated, in this section best number of divisions for different values of doppler frequency is derived such that the maximum probability of detection and the minimum average time of acquisition are obtained, as can be seen in Fig. 9, when the number of divisions increases, the average time of acquisition is not necessarily reduced. So, assuming the given estimation of Doppler frequency as follows, the best divisions are calculated with regard to parameters of acquisition system and received signal to noise ratio, as well. The critical Doppler frequency for the current N_s is shown as $f_d^{N_s}$ and defined as: critical Doppler frequency for the current N_s is the frequency that if the Doppler frequency estimation $f_d^{N_s}$ exceeds, then one additional division must be added to obtain the maximum probability of detection, or in simple words, $f_d^{N_s}$ is the frequency that determines the boundary between two consequent divisions, N_s and N_{s+1}. Equation (25) is used to calculate $f_d^{N_s}$. According to (25) the following statement shows the detection probability of a phase code for SZP algorithm with N_s divisions:

$$P_{D,N_s}^{(sc)} = \int_{V_t}^{-\infty} f_\gamma(t|H_1)dt = 1 - F_\gamma(t|H_1) \tag{41}$$

if, $Q(x) = \int_{-\infty}^{x} e^{-t^2}dt$, then

$$P_{D,N_s}^{(sc)} = 1 - Q(\frac{V_t^{N_s} - \mu_\gamma^{N_s}}{\sigma_\gamma^{N_s}}) \tag{42}$$

where, $V_t^{N_s}$ is threshold, $\mu_\gamma^{N_s}$ is the average, $\sigma_\gamma^{N_s}$ is standard deviation of $f_\gamma(t|H_1)$ with N_s number of divisions. To obtain the critical frequency of N_s divisions, the detection probability of a phase code in N_s divisions shall be equalized to the detection probability of a phase code in divisions with one

additional division, i.e. N_{s+1}, to acquire the point of intersection. Location of the intersection point is the desired critical frequency:

$$P_{D,N_s} = P_{D,N_s+1} = 1 - Q\left(\frac{V_t^{N_s} - \mu_\gamma^{N_s}}{\sigma_\gamma^{N_s}}\right) = 1 - Q(\frac{V_t^{N_s+1} - \mu_\gamma^{N_s+1}}{\sigma_\gamma^{N_s+1}}) \tag{43}$$

and finally, for the above equation, we must have:

$$\frac{V_t^{N_s} - \mu_\gamma^{N_s}}{\sigma_\gamma^{N_s}} = \frac{V_t^{N_s+1} - \mu_\gamma^{N_s+1}}{\sigma_\gamma^{N_s+1}} \tag{44}$$

V_t can be obtained from (20) and σ_γ and μ_γ can be obtained from (24). f_d can be represented by equation (22) by writing the first 5 element of $sinc(x)$ Taylor expansion (Taylor expansion of $sinc(x)$ function is: $sinc(x) = 1 - \frac{\pi^2 x^2}{3!} + \frac{\pi^4 x^4}{5!} - \cdots$). Solving (44) to obtain $f_d^{N_s}$is as follows:

$$A(f_d^{N_s})^8 + B(f_d^{N_s})^6 + C(f_d^{N_s})^4 + D(f_d^{N_s})^2 + E = 0 \tag{45}$$

where,

$$
\begin{aligned}
A = &0.5 * b_1 b_2 b^2 a_4 a^6 + b_1 b_2 b^4 a^4 a_4 + 0.5 * b_1 b_2 b^6 a^2 a_6 - 0.5 * b_4 b^2 a^6 a_1 a_2 \\
&- b_4 b^4 a_1 a_2 a^4 - 0.5 * b_4 b^6 a_1 a_2 a^2 - b_2^2 b^8 a_3 - b_2^2 b^8 a_4 + b_4 a_2^2 a^8 \\
&+ a^8 a_2^2 b_3 + 0.5 * b_4 b^6 a_2^2 a^2 - 0.5 * b_2^2 b^2 a_4 a^6 + 3 * b_4 b^2 a_2^2 a^6 - 2.5 \\
&* b_2^2 b^4 a_4 a^4 + 2.5 * b_4 b^4 a_2^2 a^4 - 3 * b_2^2 b^6 a_4 a^2
\end{aligned} \tag{46}
$$

$$
\begin{aligned}
B = &-1.5 * b_1 b_2 a_4 a^6 + 1.5 * b_4 b^6 a_1 a_2 + 1.5 * a^6 a_2 a_1 b_4 - 8 * b_1 b_2 b^4 a^2 a_4 + 18 \\
&* b_2^2 b^4 a_4 a^2 + 1.5 * a^6 a_2 a_1 b_3 + 8 * b_2^2 b^2 a^4 a_4 - 9.5 * a^6 a_2^2 b_3 + 8 \\
&* b_4 b^4 a_1 a_2 a^2 - 8 * b_1 b_2 b^2 a^4 a_4 - 9.5 * a^6 a_2^2 b_4 + 9.5 * b_2^2 b^6 a_4 - 1.5 \\
&* b_1 b_2 b^6 a_3 - 18 * b_4 b^2 a_2^2 a^4 - 8 * b_4 b^4 a_2^2 a^2 + 9.5 * b_2^2 b^6 a_3 - 1.5 \\
&* b_1 b_2 b^6 a_4 + 8 * b_4 b^2 a_1 a_2 a^4
\end{aligned} \tag{47}
$$

$$
\begin{aligned}
C = &24 * b_1 b_2 a_4 a^4 + 60 * b_1 b_2 b^2 a_4 a^2 + 54 * a^4 a_2^2 b_3 + 54 * a^4 a_2^2 b_4 - 12 * b_2^2 a_4 a^4 \\
&+ 24 * b_1 b_2 b^4 a_4 - 24 * a^4 a_2 a_1 b_3 - 60 * b_4 b^2 a_1 a_2 a^2 + 24 * b_1 b_2 b^4 a_3 \\
&+ 12 * b_4 b^4 a_2^2 - 60 * b_2^2 b^2 a_4 a^2 - 54 * b_2^2 b^4 a_4 - 24 * b_4 b^4 a_1 a_2 - 24 \\
&* a^4 a_2 a_1 b_4 + 60 * b_4 b^2 a_2^2 a^2 - 54 * b_2^2 b^4 a_3 - 12 * b_1^2 a_4 a^4 + 12 \\
&* b_4 b^4 a_1^2
\end{aligned} \tag{48}
$$

$$
\begin{aligned}
D = &-180 * b_1 b_2 a_4 a^2 - 180 * a^2 a_2^2 b_3 + 90 * b_1^2 a_4 a^2 - 180 * b_1 b_2 b^2 a^3 - 180 * a^2 a_2^2 b_4 \\
&+ 90 * b_2^2 a_4 a^2 + 180 * b_2^2 b^2 a_4 - 90 * b_4 b^2 a_1^2 + 180 * b_4 b^2 a_1 a_2 + 180 \\
&* b_2^2 b^2 a_3 - 90 * b_4 b^2 a_2^2 + 180 * a^2 a_2 a_1 b_3 - 180 * b_1 b_2 b^2 a_4 + 180 \\
&* a^2 a_2 a_1 b_4
\end{aligned} \tag{49}
$$

$$
\begin{aligned}
E = &-270 * b_1^2 a_4 - 270 * b_2^2 a_3 - 270 * b_2^2 a_4 + 540 * b_2 b_1 a_4 - 540 * b_3 a_1 a_2 - 540 \\
&* b_4 a_1 a_2 + 540 * b_1 b_2 a_3 + 270 * b_4 a_2^2 + 270 * b_3 a_1^2 + 270 * b_3 a_2^2 + 270 \\
&* b_4 a_1^2 - 270 * b_1^2 a_3
\end{aligned} \tag{50}
$$

and

$$a = \frac{\pi N}{2 f_s (N_s + 1)} \tag{51}$$

$$a_1 = V_t^{N_s+1} - \sigma^2 N \tag{52}$$

$$a_2 = \frac{N^2}{4(N_s + 1)} \tag{53}$$

$$a_3 = \frac{\sigma^4 N^2}{N_s} \tag{54}$$

$$a_4 = \frac{\sigma^2 N^3}{2(N_s + 1)^2} \tag{55}$$

$$b = \frac{\pi N}{2 f_s (N_s)} \tag{56}$$

$$b_1 = V_t^{N_s} - \sigma^2 N \tag{57}$$
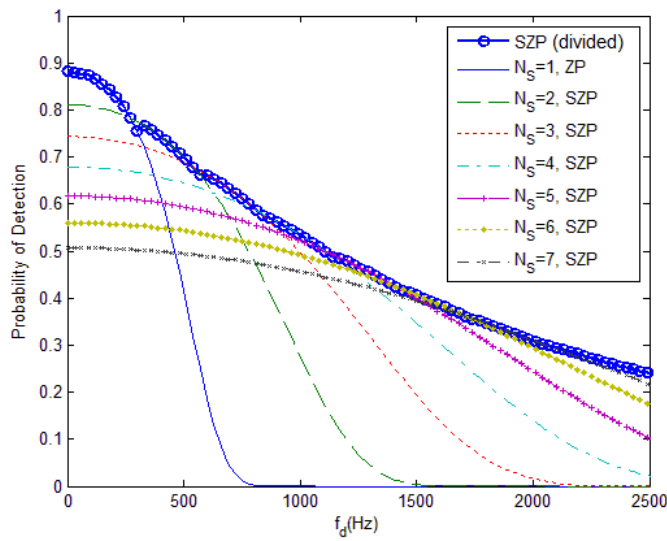
$$b_2 = \frac{N^2}{4(N_s)} \tag{58}$$

Fig. 10. Probability of detection for different values of Doppler frequencies and N_s at signal-to-noise ratio of -25dB compared with SZP algorithm with best N_s due to probability of detection

$$b_3 = \frac{\sigma^4 N^2}{N_s} \tag{59}$$

$$b_4 = \frac{\sigma^2 N^3}{2(N_s)^2} \tag{60}$$

Among eight results of (45) the desired answer is the positive, real one, larger than $f_d^{N_s-1}$ and smaller than Doppler frequency of maximum attenuation, i.e. $f_s N_s \big/ (2N)$.

Assuming that the estimation of $\widehat{f_d}$ from Doppler frequency is available, the best division method will be so that, first the critical frequency is calculated for $N_s = 1$, and if $\widehat{f_d} < f_d^1$, the system will continue with $N_s = 1$, and if not, the critical frequency is calculated for $N_s = 2$, in this case if $\widehat{f_d} < f_d^2$, the system continues to work with $N_s = 2$, and if not, the critical frequency is calculated for $N_s = 3$ and the above routine will continue. Fig. 10 shows the detection probability of SZP algorithm with best N_s in comparison with ZP algorithm SZP algorithm with constant N_s at the signal to noise of -25dB. As can be seen at Doppler frequency of approximately 300Hz the detection probability of ZP algorithm is lower than that of SZP algorithm with $N_s = 1$, thus, the frequency of 300Hz is the critical frequency for this division and for frequencies greater than that, one additional division must be added. This procedure also runs for higher stages, as a result, for instance, the detection probability of 0.5 occurs for ZP algorithm at Doppler frequency of 460Hz, for SZP algorithm with $N_s = 2$ at Doppler frequency of 780Hz but for SZP algorithm with best N_s at Doppler frequency of 1.1KHz, which represents the very good resistance of SZP algorithm with best N_s to Doppler frequency.
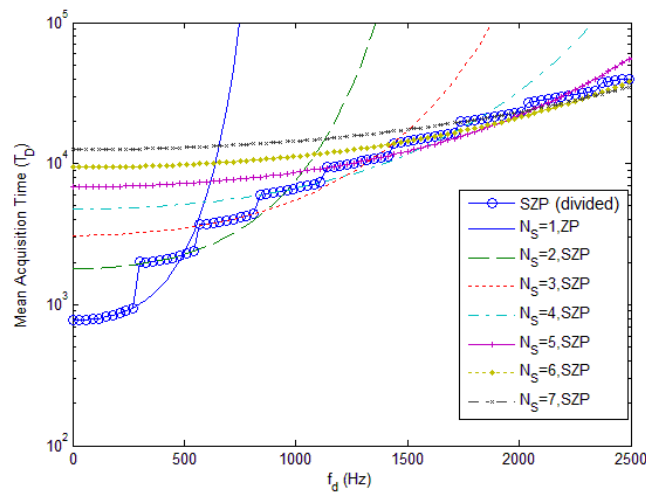

Fig. 11. The average time of acquisition for different values of Doppler frequencies and N_s at signal-to-noise ratio of -25dB with SZP algorithm with best divisions for maximum detection probability
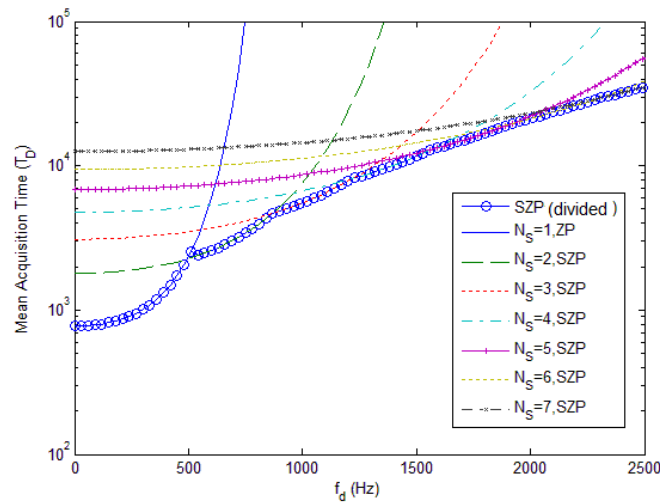
Fig. 12. The average time of acquisition for different values of Doppler frequencies and N_s at signal-to-noise ratio of -25dB with SZP algorithm with best divisions for average time of acquisition

Fig. 11 shows the average time of acquisition for the system shown in Fig. 10. As can be seen in the figure, for example, at the Doppler frequency of 600Hz, the average time of acquisition for ZP algorithm is 6,000 times more than T_D, for SZP algorithm with $N_s = 2$ is 2600 times more than T_D and for SZP algorithm with best N_s is 3,700 times more than T_D.

The reason for higher amounts of the average time of acquisition in SZP algorithm with best N_s is that in (39) the probability of detection was just addressed and imposing additional computations on system due to increase in the number of divisions, were not considered. Because of the application of the acquisition system, the criteria division can be performed for detection probability and we do that by (39) or the criteria division can be performed for average time of acquisition that the critical Doppler frequencies can be obtained using (36) and as follows:

$$E\left(T_{ACQ}\right)_{N_s} = E\left(T_{ACQ}\right)_{N_s+1} \tag{٦١}$$

where, $E\left(T_{ACQ}\right)_{N_s}$ is the average time of acquisition for N_s divisions. By solving (61) the critical frequencies for criteria division of divisions for average time of acquisition will be obtained. Fig. 12 shows the average time of acquisition of SZP algorithm when the divisions has been done for minimum time of acquisition, compared with ZP algorithm, and SZP algorithm with constant divisions. Unlike the average time of acquisition of SZP algorithm with best divisions in Fig. 11, the algorithm always has the lowest average time of acquisition in Fig. 12.

VI. CONCLUSION

In this paper, the SZP for the acquisition of spread spectrum systems with long code presented. Using SZP algorithm, resistance of acquisition against the damaging effects of Doppler frequency increases. As mentioned in section IV, at very low Doppler frequencies, using SZP algorithm with

constant divisions due to the imposition of additional computational load to the system is not recommended. However, at high Doppler frequencies using SZP algorithm increases the probability of detection and reduces the average time of acquisition. In the section V, according to the fact that SZP algorithm with specified N_s, shows different results at different Doppler frequencies, a method to determine the number of divisions was presented by which the SZP algorithm was modified for maximum probability of detection and the results were compared with those of ZP algorithm. Then, a strategy was presented to obtain the minimum average time of acquisition, by which the number of divisions was determined at each Doppler frequency. The SZP algorithm can be used as a basis for algorithms to reduce the uncertainty space Like DAM (Direct Average Method) and XFAST and Dual Folding.

REFERENCES

[1]   E. D. Kaplanand C. J. Hegarty (ed.), *Understanding GPS: Principles and Applications. Norwood*, MA: Artech House Publishers, 2006.

[2]   R. Pickholtz., D. Schilliing, and L. Milstein, "Theory of spread spectrum communications a tutorial," *IEEE Trans. Commun.*, vol. 30, pp. 855-884, May 1982

[3]   U. Cheng, W. J. Hurd, and J. I. Statman, "Spread spectrum code acquisition in the presence of Doppler shift and data modulation," *IEEE Trans. Commun.*, vol. 38, no. 2, pp.241-250, Feb. 1990.

[4]   A. Polydoros and G. L. Weber, "A unified approach to serial search spread-spectrum code acquisition part I & II," *IEEE Transaction. Commun* , vol. 32, no. 5, pp. 542-560, May 1984.

[5]   D. J. R. V. Nee and A. J. R. M. Coenen, "New fast GPS code acquisition technique using FFT," *IET Electronics Letters,* vol. 27, no. 2, pp. 158-160, 1991.

[6]   J. Pang, "Direct global positioning system P-code acquisition field programmable gate array prototyping," Ph.D. dissertation, Ohio University, 2003.

[7]   C. Yang, M. J. Vasquez, and J. Chaffee, "Fast direct P(Y)-code acquisition using XFAST," *in Proc. ION GPS,* Nashville, TN, 1999, pp 317-324.

[8]   H. Khaleghi Bizaki, M. Jabbarian Jahromi, "Compensation of the Doppler effect by the segmented matched filter in the mixer array and radar receiver," *Majlesi Journal of Electrical Engineering*, no. 2, 2008

[9]   S. W. Golomb, *Shift Register Sequences*. San Francisco, CA: Holden Day, 1967.

[10] J. G. Proakis, *Digital Communications*, 4th ed. New York: McGraw-Hill, 2000

[11] S M Ross, *Introduction to Probability models*, Academic Press; 10th ed., 2009

[12] H. Li, M. Lu, X. Cui, "Generalized Zero-Padding Scheme for Direct GPS P-code Acquisition", *IEEE Trans. on wireless commun,* vol. 8, no. 6, June 2009.